ISRM International Symposium
Eurock 2025 – Expanding the Underground Space
Trondheim, Norway, 16-20 June
ISBN 978-82-8208-079-8

Realistic Modelling of Grouted Rebar Rockbolts using 2D Finite Element Method

C.P. Fischer & M.S. Diederichs
Department of Geological Sciences and Geological Engineering, Queen's University, Kingston, Canada
caitlin.fischer@queensu.ca

B. Forbes
BGC Engineering Inc., Kingston, Canada

Abstract

Built-in numerical rockbolt models are available to practitioners conducting underground excavation design using modern numerical modelling software. The ability to predict remaining support capacity against load-, strain-, or displacement-based limits relies on the ability of the numerical bolt model to accurately represent loading and deformation mechanics.

In this research, fully grouted rebar rockbolts are modelled at laboratory- and tunnel-scale using the 2D Finite Element Method (FEM) program RS2. Two rockbolt models are compared and calibrated to laboratory-scale, pre-yield, fiber-optic pull test data. Bolt models include a "Fully Bonded" model, that is coupled with infinite stiffness to the rockmass, and a "Swellex / Split Set" model (termed the "Elasto-Plastic Interface model" in this paper), that applies a deformable interface between the rockbolt and the rockmass. Bolt models are assigned input parameters from manufacturer specifications and literature review to assess pre-yield rockbolt load development and displacement. To improve bolt model performance, the bond shear stiffness (B.S.S.) parameter in the Elasto-Plastic Interface model is calibrated.

The calibrated pre-yield Elasto-Plastic Interface model is implemented at tunnel-scale to verify mechanistic behaviours in interaction with multiple discrete loading structures. Post-yield behaviour for the shaft and the interface are approximated using elasto-plastic strength criteria. The calibrated model well represents tunnel-scale behavioural mechanisms, as exemplified through comparison to in-situ fiber-optic CT-bolt data. Realistic load development lengths, shear stress distributions, and overlapping influence zones are generated by the calibrated model.

It is recommended to model fully grouted rebar rockbolts using a pre-yield calibrated B.S.S. in the RS2 Elasto-Plastic Interface model. The calibrated B.S.S. of 5850 MN/m/m applied in this work is significantly higher than values found otherwise in the literature, but is required to accurately represent rockbolt loading and deformation mechanics. Similarly elevated B.S.S. values should be anticipated for modelling related bolt types using the RS2 Elasto-Plastic Interface model.

Keywords

Fully Grouted Rebar Rockbolts, Axial Pull Testing, Rockbolt Numerical Modelling, Finite Element Method

ISRM

1 Introduction

Grouted rebar rockbolts are widely used in civil and mining engineering to control rockmass displacements and improve excavation stability through functioning principles of rock reinforcement and holding (e.g., Farmer 1975; Hoek 2007). Grouted rebar rockbolts restrain rock deformation as they are loaded in-situ by continuous and discontinuous rock movements (e.g., Dight 1982; Hyett et al. 1996; Li and Stillborg 1999; Grasselli 2005).

1.1 Objectives and Scope

This research aims to practically and realistically model fully grouted rebar rockbolts using the 2D Finite Element Method (FEM) program RS2 by Rocscience, selected due to program accessibility and popularity in hard rock modelling. Two rockbolt models are applied and compared to Forbes (2020a) laboratory pull test data with initialized input parameters based on manufacturer specifications and literature review. Bolt model performance is assessed for representativeness of exponential load decay, load development, and displacement. The Elasto-Plastic Interface model is then calibrated to Forbes (2020a) data and implemented at tunnel-scale in interaction with discrete rockmass structure. Model behaviour is compared to in-situ fiber-optic data from Forbes (2020b), and practical recommendations for realistically modelling fully grouted rebar rockbolts in RS2 are ultimately delivered.

1.2 Numerical Rockbolt Models

RS2 provides multiple structural elements (rockbolt models) that consist of one-dimensional deformable elements that pass through the FEM mesh. RS2 rockbolts interact with modelled joints according to bolt-joint interaction theory by Rocscience technical user manuals (n.d.), incorporating principles from Dight (1982) and Grasselli (2005). Where a rockbolt crosses a joint, the section of impacted bolt (i.e., the length between two plastic hinges) is assumed to be two diameters in length. A dowel force is calculated that resists joint movement, and the bolt segment crossing the joint fails if the dowel force exceeds shear strength (assumed to be 50% of tensile strength). The RS2 rockbolt models applied in this research are described in Sections 1.2.1 and 1.2.2.

1.2.1 Fully Bonded Model

The Fully Bonded model is discretized at intersections with the FEM mesh. Each segment acts independently of others, influencing other segments only through impact on the rockmass. Axial force (F_e) in the bolt is determined from the elongation of the bolt element (Δu_e), considering bolt area (A), bolt element length (L_e), and bolt modulus (E), per Eq. (1). If axial force exceeds axial strength, bolt force is set to residual for the segment. Rock-grout and grout-bolt interfaces have infinite stiffnesses (the bolt is fully bonded to the rock, and displacement in the bolt equals that in the rock). Fully Bonded bolt discretization and axial force generation are displayed schematically in Fig. 1.

$$F_e = \frac{AE}{L_e}\Delta u_e \tag{1}$$

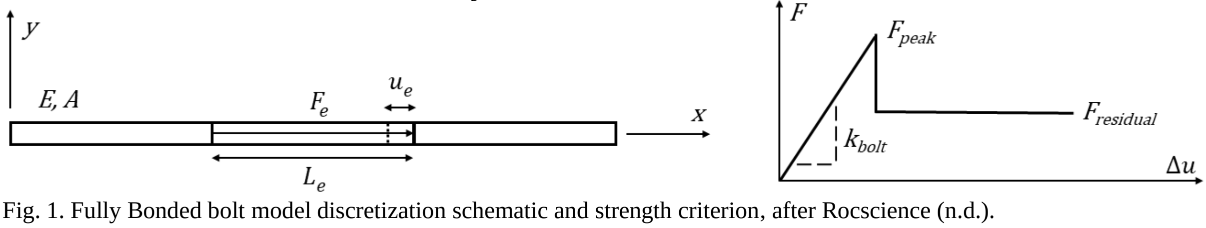

Fig. 1. Fully Bonded bolt model discretization schematic and strength criterion, after Rocscience (n.d.).

1.2.2 Elasto-Plastic Interface Model

The Elasto-Plastic Interface model is also discretized at intersections with the FEM mesh, but each bolt segment directly impacts the next. Shear force develops due to relative movement between the bolt and the rockmass according to springs of assigned B.S.S. Load transfer mechanics are complex and are detailed fully in the Rocscience technical user manuals (n.d.). The bolt equilibrium equation is written per Eq. (2), where $F_{interface}$ is shear force per unit length, u_x is segment displacement, and x is segment length. Shear force develops as a linear function of relative movement between the rock (u_r) and the bolt (u_x) according to interface stiffness ($k_{interface}$) (Eq. (3)). Bolt segments are not directly connected to the element vertices and as such, a mapping procedure is used to transfer rockbolt impact to rockmass element vertices. If axial force exceeds bolt axial strength, bolt force is set to residual. Similarly, if bond strength (B.S.) is exceeded, bond force is set to residual. The title "Elasto-Plastic Interface" model is applied in this work, as residual strength is assigned to equal peak strength. In RS2, post-yield strengthening or weakening to a constant value may instead be applied.

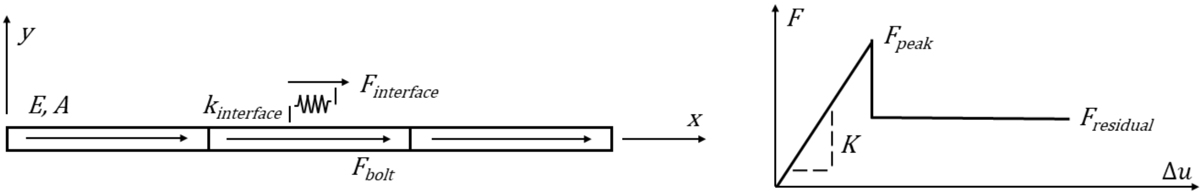

Fig. 2. Elasto-Plastic Interface bolt model discretization schematic and strength criterion, after Rocscience (n.d.). The strength criterion schematic applies separately to both the bolt shaft and the bond interface.

$$F_e = \frac{AE}{L_e} \Delta u_e \tag{2}$$

$$F_{interface} = k_{interface}(u_r - u_x) \tag{3}$$

2 Fiber-Optic Axial Testing Data

Forbes et al. (2017, 2018) developed, refined, and tested a fiber-optic instrumentation technique for rockbolts that consists of embedding and encapsulating a single mode optical fiber within shallow grooves machined along the length of a rebar shaft. The applied Luna Innovations (2019) interrogator can measure strain at a discrete measurement interval spacing as low as 0.65 mm along a fiber optic sensor (FOS). The experimental axial pull test data referenced in this research is from a 19.5 mm diameter, 1.15 m long, grouted rebar rockbolt specimen (titled "RC31-1000" in Forbes 2020a). RC31-1000 results compare well to grouted rebar experimental results in the literature (e.g., Li et al. 2016). Forbes (2020a) test setup is shown in Fig. 3. Load is applied to the rebar free length at a displacement-controlled rate of 1 mm/min, up to 100 kN (falling beneath the 120 kN yield load of the rebar).

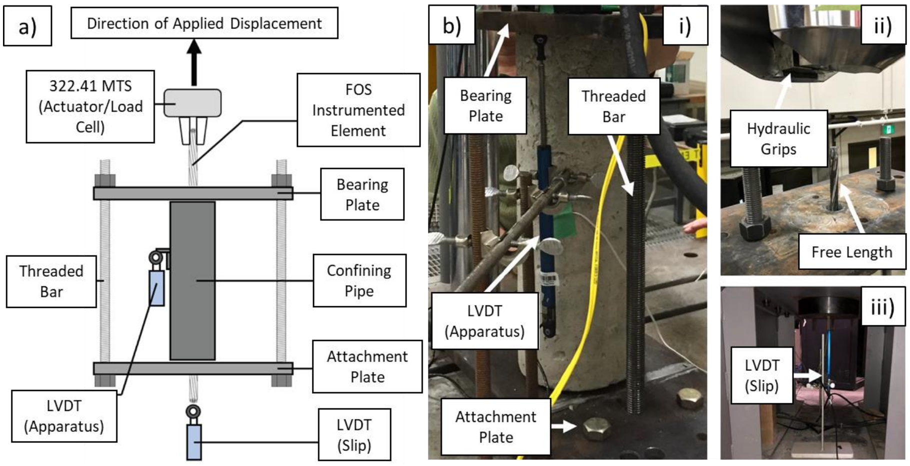

Fig. 3. Schematic and photographs of the rebar axial pull testing setup (after Forbes 2020a). The rebar is cement-grouted into a precast 31 mm center, within a 200 mm diameter concrete cylinder. The FOS is embedded within lengthwise, diametrically opposed square grooves machined along the rebar length (3.0 mm by 3.0 mm). The specimen is constrained between two steel plates, and 0.15 m of rebar free length extends through a hole in the top plate.

Axial strain is measured continuously by the FOS and is reported as an average calculated from diametrically opposing positions along the FOS to compensate for bending moment induced strain. Strains are converted to deformations (δ) per Eq. (4), by integrating axial strain along the grouted length of the test specimen, beginning at the toe, where Δx is the spatial resolution of the FOS (0.65 mm). Axial strain is converted to axial load using Eq. (5), where A is the cross-sectional area of the rebar, and E is the Young's Modulus of the rebar. The interfacial shear stress (τ_{int}) between the rebar and grout is calculated using Eq. (6), where r is the rebar radius and i refers to the position along the FOS at increments of Δx (Farmer 1975).

$$\delta = \int_{End\ of\ FOS}^{Start\ of\ FOS} \varepsilon_{axial}(\Delta x) \tag{4}$$

$$F_{axial} = \varepsilon_{axial} AE \tag{5}$$

$$\tau_{int} = \frac{rE}{2\Delta x}(\varepsilon_{axial,i+1} - \varepsilon_{axial,i-1}) \tag{6}$$

3 Laboratory-Scale Rockbolt Model Input Parameters

The laboratory-scale model geometry is presented in Fig. 4. The 1.15 m long rebar is oriented vertically, with its lower 1 m embedded in a concrete material (properties in Table 1), with pin boundary conditions. In RS2, rockbolt segments cannot exist outside of a defined material volume, nor can axial load be applied directly to the end of the Fully Bonded bolt model. As such, the rebar free length (0.15 m) is simulated in a low stiffness material, separated from the concrete by a low stiffness joint. Axial loading is initiated in the rockbolt using a displacement boundary condition applied to the top of the low stiffness material. Load develops uniformly in the free bolt length, thus adequately simulating behaviour. Applied displacement is increased incrementally in five stages: 0%, 25%, 50%, 75%, and 100% of final displacement required to achieve 100 kN in the bolt's loaded end.

Bolt diameter, area, steel modulus, and tensile capacity are initialized using manufacturer specifications, while B.S. and B.S.S. for the Elasto-Plastic Interface model are initialized using parameters from the literature (Table 2). Fischer and Diederichs (2023) identified a parametric range of approximately 0.2 to 0.8 MN/m for B.S. based on a variety of pull tests (e.g., Li et al. 2016). A B.S. of 0.8 MN/m is selected to represent high-quality grouting achieved in the Forbes (2020a) test. Fischer and Diederichs (2023) identified estimates of B.S.S. in the literature ranging from approximately 10 to 100 MN/m/m. An initial B.S.S. of 100 MN/m/m is selected for this work.

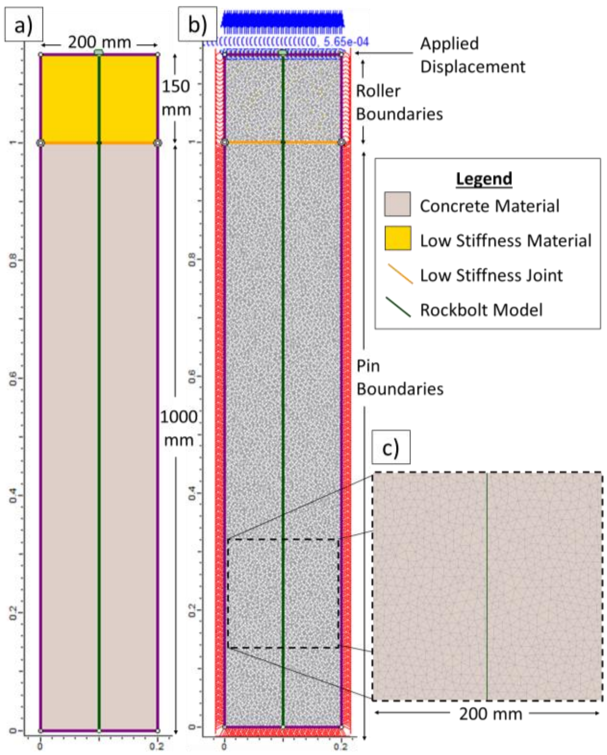

Fig. 4. RS2 model geometry after Forbes (2020a) axial pull test. a) Unmeshed, simple geometry. b) Mesh and boundary conditions, showing 10,000 uniform, six-noded mesh elements. c) Mesh inset.

Table 1. RS2 model material and joint input parameters for the Forbes (2020a) axial pull test.

Parameter	Concrete Material	Low Stiffness Material	Low Stiffness Joint
Young's Modulus (MPa)	15,600	0.001	N/A
Poisson's Ratio	0.17	0.25	N/A
Normal Stiffness (MPa/m)	N/A	N/A	0.001
Shear Stiffness (MPa/m)	N/A	N/A	0.001
Strength Model	Elastic	Elastic	Elastic

Table 2. Initial bolt model inputs for the Fully Bonded and Elasto-Plastic Interface models.

Parameter	Fully Bonded Model	Elasto-Plastic Interface Model
Bolt Diameter (mm)	19.5	19.5
Tributary Area (mm^2)	285	285
Bolt Modulus (MPa)	200,000	200,000
Tensile Capacity (MN)	0.120	0.120
Bond Strength (B.S.) (MN/m)	N/A	0.8
Bond Shear Stiffness (B.S.S.) (MN/m/m)	N/A	100

4 Laboratory-Scale Model Results

Axial load and displacement results for the Fully Bonded and Elasto-Plastic Interface models using input parameters from Table 2 are presented with the Forbes (2020a) data in Fig. 5.

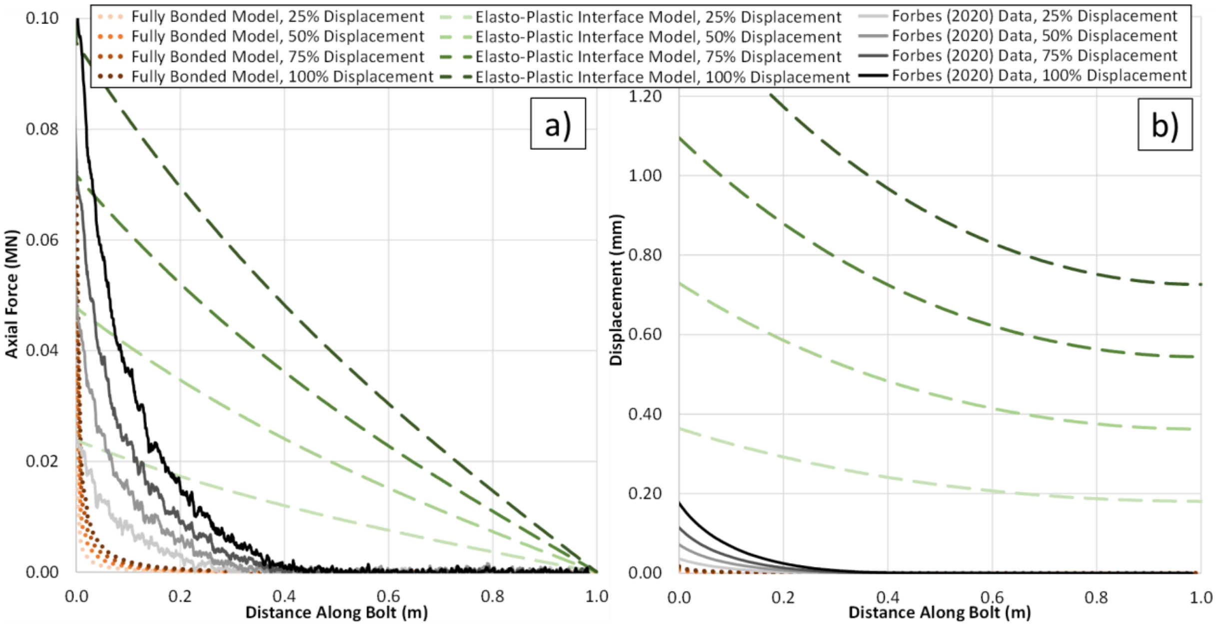

Fig. 5. a) Bolt axial load and b) bolt axial displacement for the Fully Bonded and Elasto-Plastic Interface bolt models at 25%, 50%, 75%, and 100% of final displacement to achieve 100 kN at the loaded bolt end, and the Forbes (2020a) data.

The Fully Bonded model greatly underpredicts load propagation and displacement towards the toe of the bolt compared to the Forbes (2020a) data (Fig. 5). Load decays exponentially along the bolt length (as per Farmer 1975; Li and Stillborg 1999), but decay is extremely abrupt, resulting in a load development length of 0.15 - 0.20 m compared to 0.40 - 0.45 m in the Forbes (2020a) data (which is corroborated by other fully grouted rebar pull test results, e.g., Li et al. 2016). These underpredictions occur due to the Fully Bonded model formulation, where the impact of a given bolt segment on the next is calculated only through impact on the rockmass, rather than on the next bolt segment itself.

Conversely, the Elasto-Plastic Interface model greatly overpredicts load development along the bolt compared to the Forbes (2020a) data, exhibiting an unrealistic load development length of the entire bolt (1.0 m), and demonstrating limited exponential load decay. Displacement is greatly overpredicted, with the entire bolt displacing towards the pulled end (i.e., non-zero displacement at the toe end). In conclusion, both bolt models, when employing manufacturer specifications and literature-reviewed parameters, poorly reflect Forbes (2020a) data.

Model calibration is therefore required to improve mechanistic performance. The B.S.S. parameter in the Elasto-Plastic Interface model is examined for calibration, as B.S. is not exceeded in pre-yield testing and therefore does not influence results. In the Fully Bonded model, no interface parameters are available for modification, and manipulating the bolt modulus has been shown to be ineffective due to the bolt model formulation (Fischer and Diederichs 2023; Fischer et al. 2024).

Results for the pre-yield calibrated Elasto-Plastic Interface model, with a B.S.S. of 5850 MN/m/m, are shown in Fig. 6. The calibrated model well represents grouted rebar behaviour in terms of load development length, exponential load decay, and displacement. The 5850 MN/m/m B.S.S. value is significantly higher than comparable values found in the literature for interface stiffness (~10 - 100 MN/m/m). The calibrated B.S.S. value is program-specific, bolt model-specific, and for rockbolt RC31-1000 (Forbes 2020a). However, these results indicate that higher B.S.S. values should be anticipated in modelling similar bolt types using the RS2 Elasto-Plastic Interface model.

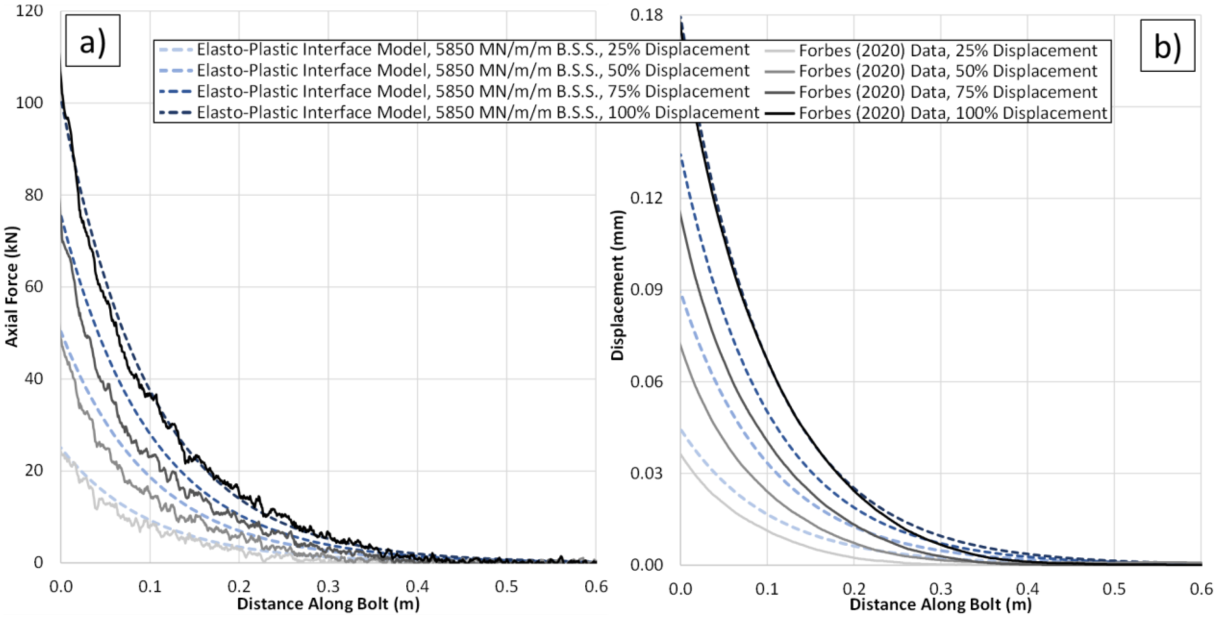

Fig. 6. a) Bolt axial load and b) bolt axial displacement for the calibrated 5850 MN/m/m B.S.S. Elasto-Plastic Interface model for 25%, 50%, 75%, and 100% of final displacement, and the Forbes (2020a) data.

5 Tunnel-Scale Rockbolt Model Input Parameters

The calibrated Elasto-Plastic Interface model (5850 MN/m/m B.S.S.) is implemented at tunnel-scale to assess model performance in interaction with discrete jointing. The tunnel-scale model consists of a 10 m diameter tunnel situated at 1 km depth in an isotropic stress field in a Geological Strength Index (GSI) 65 rockmass (Hoek et al. 2002) (Fig. 7). The tunnel is excavated in five stages: the first stage is unexcavated, the second stage is excavated with 100% induced stress load applied to the tunnel boundary, and the third, fourth, and fifth stages have 40%, 5%, and 0% induced stresses applied to the excavation boundary, respectively. 5 m long rockbolts are installed in 45-degree increments around the tunnel at the face (40% support pressure) and are loaded passively. 3-noded mesh is graded denser towards the explicit rockmass zone, with an average element length of 0.25 m around the excavation. The mesh is further densified around the support element presented in this analysis (bolt B1 in the roof), with an average element length of 0.10 m along B1.

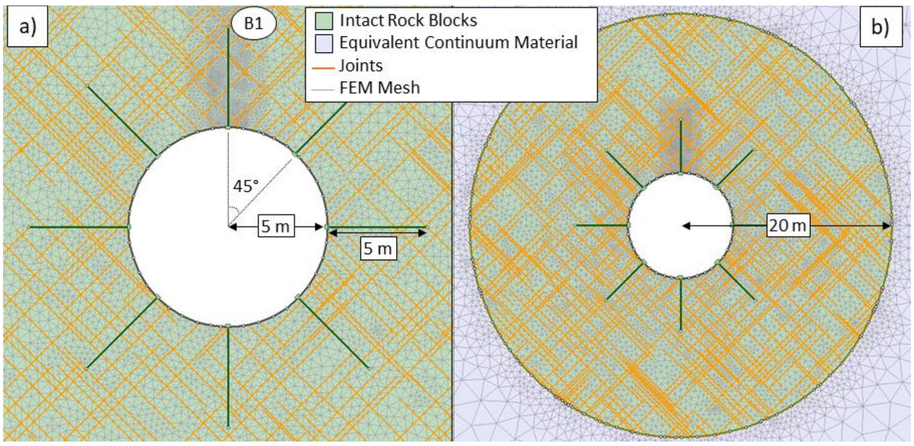

Fig. 7. a) Excavated tunnel in an explicitly modelled GSI 65 rockmass. "B1" indicates the bolt in the roof. b) Zoomed-out image of the explicit rockmass zone in the equivalent-continuum material, extending to pinned external boundaries.

The tunnel-scale model is developed using the Fischer and Diederichs (2024) methodology for explicitly modelling rockmasses of a given GSI using explicit joint networks and intact rock blocks. An elasto-plastic strength criterion is defined for the intact rock blocks using the Generalized Hoek-Brown strength criterion (Hoek et al. 2002). Joint density, 2D inclination, finite trace length, and number of joint sets are defined according to Fischer and Diederichs (2024) (Table 3).

Post-yield fully grouted rebar model behaviour is approximated using an elasto-plastic criterion for the shaft and interface, such that the bolt may continue to deform while maintaining near-peak load prior to ultimate yield (Hoek 2007). Bond strength has been shown to follow a tri-linear failure envelope (Ren et al. 2010), which is not implementable in the RS2 bolt model. It is worth noting that in RS2, bolt yield indicators are generated at peak load, and therefore, ultimate rockbolt rupture must be assessed through manual comparison to project-specific rockbolt strain- or displacement- limits.

Table 3. Explicit rockmass model input parameters developed using the Fischer and Diederichs (2024) methodology.

Intact Rock Block Input Parameters		**Baecher Joint Network Input Parameters**	
UCS (MPa)	120	Density (joints/m)	1.0
Intact Young's Modulus, E_i (GPa)	35.0	Inclinations, 2 Sets in Plane (°)	45, -45
Unit Weight (MN/m^3)	0.027	Trace Length (m)	8.1
m_i	25	JCS (MPa)	48.8
Poisson's Ratio, v	0.25	JRC	12
GSI	85	Base Friction Angle (°)	30.3
		Normal Stiffness, K_n (MPa/m)	90,000
		Shear Stiffness, K_s (MPa/m)	22,400

6 Tunnel-Scale Model Results

Results from bolt B1 in the tunnel-scale model are demonstrated in Fig. 8. Model results are assessed for realism in terms of mechanistic behaviour through comparison to in-situ FOS-instrumented CT-bolt data from Forbes (2020b). Forbes (2020b) installed CT-bolts in an active tunnel operation in the Hawkesbury Sandstone in Sydney, Australia. Although CT-bolts have a longer critical embedment length than fully grouted rebar, the in-situ data is useful for mechanistic comparison.

Fig. 8 and Forbes (2020b) data (not pictured) both display local axial load maxima at discrete feature intersections (neutral points, per Freeman 1978). On opposing sides of a neutral point, a pickup length resists rockmass movement towards the excavation, and an anchor length anchors the element deeper ground. These shear stress inflections are shown both by the calibrated model (Fig. 8) and Forbes (2020b) data. Overlapping influence zones are also noted in both datasets, as expected from discrete loading features that fall within two critical embedment lengths of one another (e.g., Hyett et al. 1996; Forbes 2020a). Additionally, the grouted rebar model showcases realistic load development lengths at each discrete loading location (Forbes 2020a; Li et al. 2016).

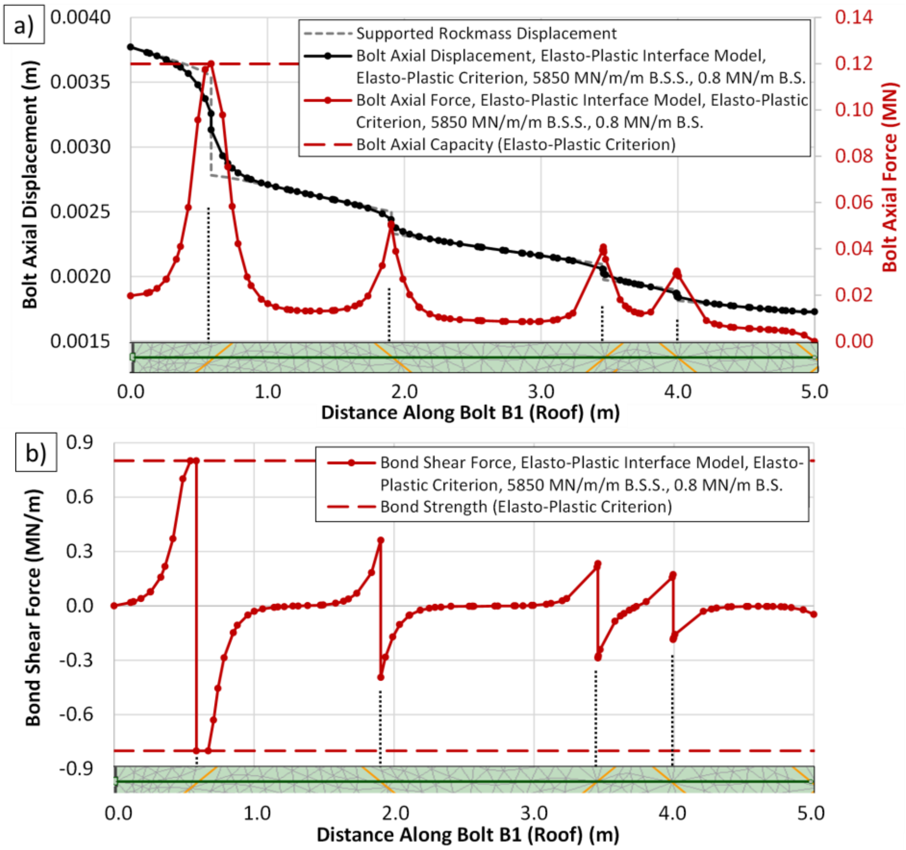

Fig. 8. a) Bolt axial displacement and bolt axial force and b) bond shear force for bolt B1 in the tunnel-scale model.

7 Conclusions

Two RS2 rockbolt model formulations (Fully Bonded and Elasto-Plastic Interface models) are applied to simulate grouted rebar rockbolt behaviour at laboratory- and tunnel-scale in RS2. Bolt models are first assigned input parameters from manufacturer specifications and literature review, and compared to pre-yield fiber-optic pull testing data from Forbes (2020a). The Fully Bonded model greatly underpredicts load development and displacement due to model formulation limitations, while the Elasto-Plastic Interface model (using initial estimates of B.S.S. and B.S.) greatly overpredicts load development and displacement. Through calibration of the B.S.S. parameter in the Elasto-Plastic Interface model, a good representation of load development length, load decay, and displacement is achieved. The calibrated B.S.S. of 5850 MN/m/m is significantly higher than values found otherwise in the literature, but is required to accurately simulate grouted rebar behaviour using the RS2 Elasto-Plastic Interface model. Similarly elevated B.S.S. values should be anticipated for modelling related bolt types using the RS2 Elasto-Plastic Interface model.

The calibrated pre-yield Elasto-Plastic Interface model also assessed at tunnel-scale in an explicitly jointed rockmass. The calibrated model demonstrates realistic load development lengths, simulations of neutral points, interfacial shear stress distributions, and overlapping influence zones, as exemplified through comparison with in-situ CT-bolt data from Forbes (2020b). Future work should include bolt models in other industry-common geotechnical software (including 3D software), other rockbolt types, considerations for shear loading, and more advanced post-yield behaviour implementation.

References

Dight PM (1982) Improvements to the stability of rock walls in open pit mines. Dissertation, Monash University

Farmer IW (1975) Stress distribution along a resin grouted rock anchor. International Journal of Rock Mechanics and Mining Sciences 12: 347–351

Fischer CP, Diederichs MS (2023) Analyzing numerical grouted rockbolt behaviour in jointed pseudo-discontinuum models. 15th ISRM Congress 2023, Salzburg, Austria, 2023

Fischer CP, Diederichs MS (2024) Elasto-Plastic and Post-Yield Weakening Jointed Rockmass Response in a Comparison of Equivalent-Continuum and Explicit Structural Models. Canadian Geotechnical Journal 61(4) https://doi.org/10.1139/cgj-2022-0190

Forbes B (2020a) Insight into the coaxial load distribution of fully grouted rebar, cable bolt, CT-Bolt, and D-Bolt reinforcement elements. Chapter 4, Dissertation, Queen’s University

Forbes B (2020b) Measuring the in-situ response of tunnel support using high spatial resolution optical fiber strain sensing. Chapter 6, Dissertation, Queen’s University

Forbes B, Vlachopoulos N, Hyett AJ, Diederichs MS (2017) A new optical sensing technique for monitoring shear of rock bolts. Tunnelling and Underground Space Technology 66: 34–46

Forbes B, Vlachopoulos N, Hyett AJ (2018) The application of distributed optical strain sensing to measure the strain distribution of ground support members. FACETS 3: 195–226

Freeman TJ (1978) The behaviour of fully-bonded rock bolts in the Kielder experimental tunnel. Tunnels and Tunnelling International 10(5): 37–40

Grasselli G (2005) 3D Behaviour of bolted rock joints: experimental and numerical study. International Journal of Rock Mechanics and Mining Sciences 42(2005): 13–24

Hoek E (2007) Rockbolts and cables. Practical Rock Engineering. https://www.rocscience.com/assets/resources/learning/hoek/Practical-Rock-Engineering-Full-Text.pdf Accessed 2024-12-12

Hoek E, Carranza-Torres C, Corkum B (2002) Hoek-Brown Failure Criterion – 2002 Edition. 5th North American Rock Mechanics Symposium, Toronto, ON, Canada, 2002, 1: 67-273

Hyett AJ, Moosavi M, Bawden WF (1996) Load distribution along fully grouted bolts, with emphasis on cable bolt reinforcement. Numerical and Analytical Methods in Geomechanics 20: 517–544

Li CC, Kristjansson G, Høien AH (2016) Critical embedment length and bond strength of fully encapsulated rebar rockbolts. Tunnelling and Underground Space Technology 59(2016): 16–23

Li CC, Stillborg B (1999) Analytical models for rock bolts. International Journal of Rock Mechanics and Mining Sciences 36(1999): 1013–29

Ren FF, Yang ZJ, Chen JF, Chen WW (2010) An analytical analysis of the full-range behaviour of grouted rockbolts based on a tri-linear bond-slip model. Construction and Building Materials 24: 361–370

Rocscience (n.d.) Bolt Support Models. https://www.rocscience.com/help/rs2/verification-theory/theory-manuals/bolts. Accessed 2024-12-12